A Biodegradable Polycaprolactone based ink developed for 3D Ink Jetting

Yinfeng He[1], Sam Kilsby[2], Chris Tuck[1], Ricky Wildman[1], Steven Christie[2], Hongyi Yang[1], Steven Edmondson[3],
[1]Additive Manufacturing and 3D Printing Research Group, Nottingham University, UK
[2]Department of Chemistry, Loughborough University, UK
[3]Materials Department, Manchester University, UK
epxyh@exmail.nottingham.ac.uk
REVIEWED

Abstract: Biomedical applications are one of the driving forces for Additive Manufacturing, however to extend the range of applications and markets new materials are required. A new type of biodegradable Polycaprolactone (PCL) based ink that is suitable for 3D inkjet printing was successfully developed. UV curable PCL was synthesized and mixed with Poly(ethylene glycol) di-acrylated (PEGDA) to prepare an ink with suitable viscosity for inkjet printing. Their mechanical properties as well as the printing accuracy were measured by nano-indentation and scanning electron microscopy. Post curing was applied to printed samples in order to study how post curing may influence sample properties. It was found that within 30min post-curing period, the sample's surface which is direct illuminated by UV light increased from 31.22MPa to 70.20MPa while the bottom surface showed less incensement from 34.9MPa to 39.8MPa.

Introduction

3D Printing or Additive Manufacturing (AM), as a disruptive manufacturing technology, has been attracting increasing attention in recent years. Many studies have been carried out to enable AM to become a process that is able to manufacture end-use products. One of the potential applications for AM is in the making of biodegradable or bioresorbable medical products with the potential of tailored drug release functions. Some biomedical products require complex and strict pore structures to achieve enhanced cell adhesion and growth [1-3]. These requirements in pore structure and sizes are difficult to be controlled with current manufacturing techniques (such as foaming). However with AM technology, the sizes and locations of each pore can be accurately controlled and this lends the possibility of being able to manufacture bespoke products.

Polycaprolactone (PCL) is widely used in biomedicine as it can gradually decompose by random hydrolytic chain scission of the ester groups [4-5]. Some researchers have attempted to build PCL structures with additive manufacturing methods such as Powder Bed Fusion (i.e. laser sintering) or material extrusion [6-8]. However, little work has been done in processing PCL by 3D inkjet printing. Compared with other AM techniques, 3D inkjet printing has the potential of producing multi-material artefacts within a single process cycle with controlled material distribution. This facility can be used to manufacture products with localized drug distribution or degradation speeds. Therefore, developing a biodegradable material which is

suitable for 3D inkjet printing could bring the manufacturing of biomedical product into a brand new field.

3D inkjet printing requires a low viscosity ink, which solidifies quickly after deposition hence photo-curing has been a popular method of achieving fast solidification for commercial materials. Although pure caprolactone does not cure under UV irradiation, groups (normally acrylated group) can be grafted onto the end of a PCL polymer chain to make it UV curable [9-10]. As printers have very strict requirements on ink viscosity, a diluent is also a necessary component to help adjust the inks viscosity. PolyEthyleneGlycol (diacrylated) (PEGDA), can be used as such a diluent, and has been widely used for UV curable biocompatible materials [11-13]. Some authors have suggested that a copolymer of PCL and PEG can help develop products with different surface function and modify the drug release profile of a material because PCL is hydrophilic and PEG is hydrophobic [14-15].

In this paper, the printability of UV curable PCL: Polycaprolactone di-methacrylated (PCLDMA) was assessed. Rheological data were collected with different PEGDA proportions in a temperature range from ambient temperature to 60ºC to help select suitable processing conditions and PEGDA concentration for printing. The synthesised UV curable PCL's viscosity was adjusted by adding 30wt% of PEGDA and successfully printed by using a Dimatix DMP2800 inkjet printer.3D structures were then created with this ink and characterized to help understand the properties of this material.

Methodology

Ink preparation

PCLDMA (synthesised) and PEGDA (Sigma-Aldrich average Mn~250) were added into an 8ml amber vial and stirred at room temperature for 15mins at 800rpm using an IKA RCT Basic IKAMAG Magnetic Stirrer (with Temperature Controller). 3wt% of photo-initiator (2,4-Diethyl-9H-thioxanthen-9-one(DETX),sigma-aldrich,98%) and 3wt% of accelerator (Ethyl 4-(dimethylamino)benzoate(EDB),sigma-aldrich,99wt%) were added into the PCLDMA:PEGDA mix and stirred at 85ºC for 5mins until all the solutes are fully dissolved. Before printing, the prepared ink required a degassing procedure to remove dissolved oxygen and to help minimize the 'oxygen inhibition' effect [17-18]. The degassing procedure was carried out by purging the mixed ink with nitrogen gas for 15minutes. This procedure created lots of Nitrogen bubbles within the ink which seriously reduces the droplet formation stability of the ink. Therefore the ink was prepared 24hrs prior to printing; the degassed ink was then settled to release the bubbles.

Printability Assessment

The key parameters for determining ‘’printability’’ are viscosity and surface tension. Normally, viscosity is the most fundamental parameter used to decide whether an ink is printable or not. The printing viscosity range varies dependent on the printheads being used. Surface tension should also be taken into consideration. It has been reported that the inverse Ohnesorge number (Oh^{-1}) can be used as the printing indicator (Z) to help predict an ink’s printability. Z takes both viscosity and surface tension into consideration and is shown following equation[16].

$$Z = \frac{\sqrt{\rho r \gamma}}{\mu}$$

Whereρ is density, r is characteristic length, γ is surface tension of the fluid and μ is viscosity of ink.

The viscosity of the PCLDMA:PEGDA mixture (under shear rates of $100s^{-1}$ and $1000s^{-1}$) was measured by a cone plate rheometer (Malvern Kinexus Pro) to identify the PCLDMA:PEGDA proportion and the processing temperature that would give a suitable viscosity for inkjet printing. Each measurement started at 25ºC with 5ºC increments up to 60ºC. A protocol of waiting 300s after reaching the test temperature was set to ensure the ink was in a steady state condition. At each temperature point and shear rate, the viscosity was recorded at 5s intervals within a 180s test time.. Surface tension was measured by a pendant drop method using a Kruss DSA100S. The shape was captured at the equilibrium state and used to calculate the surface tension.

Sample properties assessment

The ink with the final composition was then injected into a print cartridge. The injection procedure was carried out in the dark to prevent light irradiation and careful attention was paid to avoid bubble formation within the ink. The cartridge was wrapped with foil tape to make sure the ink was not cured inside the cartridge by ambient light. About 2ml of the prepared ink was injected into a disposable cartridge and printed by DimatixDMP-2800 material printer. The printed ink was cured by real-time UV curing; a UV curing unit was mounted directly on to the printing unit (Figure 1) to move in conjunction with the print direction. A further UV LED unit (intensity of $1000mW/cm^2$) was used to examine the influence of different post-curing time (10 minutes, 20 minutes and 30 minutes) on the mechanical properties of the printed parts.

The mechanical properties of printed sample were characterized by nano-indentation at room temperature (Micro Materials, NanoTest NTX with hot stage and inert gas cabinet). Both the top and bottom surface were characterized. Load-depth curves were recorded on 5×5 grid with 100μm separation between each indentation. The

applying force was set to 5mN with a 0.25mN/s loading and unloading rate and a spherical indenter with 50μm radius was used. The Hardness is calculated by:

$$\mathrm{H} = \frac{P}{A} = \frac{P}{\pi {a_r}^2}$$

Where P is applied load, a is the radius of the circle of contact. The radius of the circle of contact is calculated by follow equation:

$$a_r = \frac{\sqrt{4R(h_t + h_r) - (h_t + h_r)^2}}{2} \cdot c$$

Where R is the radius of the spherical indenter,,h_t is the total penetration depth,h_r is the residual depth and c is correction constant for piling-up or sinking-in effect [19],

The indentation modulus E can be calculated by:

$$\mathrm{E} = \frac{3}{4}\frac{P}{a_r h_e}$$

Where P and a are applied load and radius of circle of contact respectively, h_e is the elastic deformation depth.

Mesh structures were printed to help understand the manufacturing accuracy that PCLDMA:PEGDA (70:30) ink could achieve. Printed mesh structures were sputter coated with Platinum and examined by SEM (XL30 ESEM Philips).

Results and Discussion

Printability Assessment

The viscosity results of PCLDMA with different PEGDA proportions were measured (Table 1). As PEGDA is a diluent and only biocompatible after curing, when choosing the composition, the amount of PEGDA needs to be as low as possible within the printable viscosity range, in order to maximise the biodegradability of final product. PCLDMA with 30wt% of PEGDA at 60ºC was chosen as the final proportion in this paper based on the rheological tests and printing requirements. However, as different printheads have different printing viscosity ranges, this does not apply to all the piezo based printheads. The viscosity distributions of PCLDMA:PEGDA mixture with various proportions under different environment temperatures are given in Table 1, which can help decide the optimum composition for the other printheads.

As PEGDA is only bio-compatible but not biodegradable material, it will reduce the biodegradability of the final product. Therefore, when choosing the final composition, the one with higher PCLDMA concentration but still within printable range is

preferred. Based on this principle, PCLDMA:PEGDA (70:30) was chosen as the final composition, which will be used for following printing.

The printability indicator, Z, for PCLDMA:PEGDA (70:30) was then calculated (Table 3). It has been suggested that when the value of the printing indicator is between 1 and 10, the ink will normally be printable [16]. From Table 2, it can be seen that based on these calculations, the Z values of PCLDMA:PEGDA (70:30) at 60 ºC were in the printable range.

The viscosity of the ink was measured throughout the whole ink preparation procedure to monitor viscosity variations (Table 3). It can be seen that after adding photo-initiators and being degassed, the viscosity of the ink increased by 5-10%. This was due to two reasons: the adding of solid content and a small amount of curing during the degassing procedure. As one may expect, adding high viscosity content will increase the viscosity of the ink. The photo-initiator and accelerator used in our experiment are both solids and they occupied 6wt% of the whole ink which led to viscosity increase. Also, the ink became quite reactive during degassing and as the degassing procedure was not carried out in a completely dark environment there will be small amount of curing which also increased the prepared ink's viscosity.

Real-time curing and Post-curing effect

Five square specimens, 5mm (W)*5mm (L), were prepared for nano-indentation testing. The printing pattern and samples are shown in Figure 3 where 100 layers were printed. The final thicknesses of these square samples were ~500μm.

The hardness and indentation modulus of printed samples with different post curing time were measured by nano-indentation (Table 4). The measurements were carried out on the sample's top and bottom surface respectively. As the samples were produced by stacking up layers of material, those layers printed in the early stages will inevitably be repeatedly exposed to UV illumination when following layers are printed. This will lead to a printed sample which has a gradient of UV exposure time from bottom to top. As UV exposure time is normally related to curing level, this may eventually result in property deviation and therefore, both surfaces were measured separately.

The indentation results (Table 4) showed the top and bottom surface of the sample has very similar properties before any post-curing treatment. The hardness and indentation modulus on both surface have variations however these are within the testing deviation range.

The mechanical properties of the sample's top surface, which was directly illuminated by UV light, had a significant increase after 10mins of post-curing (Table 4 and Figure 4).However additional post-curing for 20mins and 30mins did not further influence these properties. The rise of hardness and modulus on the top surface after post-curing was mainly due to and increase of cross-link density. Prior work has shown that the hardness and modulus of a crosslink material is positive in relation to its crosslink density [20, 21]. At low crosslink density, polymer chains are

less restricted, therefore it can easily deform with an applied manifesting as a low hardness and modulus. As crosslink density increases those free segments are connected with each other building an increasingly dense network. The mobility of the polymer chain segments becomes restricted and the specimen will then show stronger resistance to an applied force. When a specimen was printed, the conversion of the C=C group into the covalent crosslink cannot normally reach 100%. During the post-curing procedure UV illumination will provide extra energy to help the residual C=C group form new crosslink and therefore, further increase the crosslink density and hence its hardness and modulus.

Meanwhile, the properties of the sample's bottom surface did not show a notable change with the increase of post-curing time. This could be because during the post-curing procedure, samples were illuminated from the top surface and the UV irradiation needs to penetrate the whole sample before reaching the bottom surface. During the penetration procedure, the intensity of the UV light would be reduced by absorption from the sample and result in only a small quantity of radiation reaching the bottom surface. From the nano-indentation results, the bottom surface did not receive enough energy to achieve further crosslinking and therefore the properties remain unchanged. UV absorbance spectrums with a different thickness of cured ink films are currently under characterization to affirm this hypothesis and also help discover the penetration depth.

Printing and Characterization

Mesh structures were then printed and a schematic figure of the printing pattern was shown in Figure 5 (a). Meshes with three different wall thicknesses (150μm, 300μm and 500μm) were printed onto glass slides for futher SEM examination. The distance between each wall was set as 1mm to allow each printed vertical or horizontal wall to be seperated from each other. Ten layers of PCLDMA:PEGDA (70:30) were printed and the sample appearance is shown in Figure 6(b).

The mesh structures were then observed under SEM (Figure 6). The actual printed wall thickness was measured and calculated to help analysing the dimensional variation between the printed structure and the original design. From the results in Table 5, it can be noticed that the printed mesh structure with larger designed wall thickness had less deviation percentage compared with the meshes with thinner walls. However the deviation was always around 40μm which would indicate that the processing accuracy of Dimatix material printer for PCLDMA:PEGDA (70:30) is around 40μm, when using printhead with 21μm nozzles.

Figure 6 also showed that under the print conditions the PCLDMA:PEGDA (70:30) ink could not form accurate and sharp edges. Rectangular gaps were designed inside the mesh structure. However in the actual printed structure, the gap morphed into rounded rectangular shapes. Meanwhile, dislocation of printed ink droplets can be observed from the SEM pictures and causing rounded rectangular gaps as well

as curving walls. These might be due to the slow curing speed of the printed ink. Although, the ink was illuminated by UV light immediately after being printed, the illumination time was quite limited in a single scan. This is becausethe UV curing unit was attached and moving with the printhead. So the energy provided in a single scanning may not be enough to allow freshly deposited ink to become fully cured immediately. Therefore, merging and dislocation of the uncured ink droplet could happen due to gravity, movement of the platform and merging with the ink deposited in subsequent printing cycles. All these will lead to rounded edge and curing walls.

However, as the illumination area of UV curing unit were larger than the printed area of each printing cycle, the previously printed ink can still receive UV illumination during the following printing. So the ink will receive discontinuous UV illumination and finally be cured after obtaining enough energy. But the curing time will be enlarged compared with continuous UV illumination. Increasing the curing speed could help printed ink cure in a shorter period of time, hence reduce the chance of merging and dislocation happening, improving the print quality. This could be achieved by either increasing the intensity of UV illumination or creatingan oxygen free environment.

Figure 6 (d) is a SEM image showing a cured mesh surface in high magnification. Wrinkles (about 1 to 2μm) can be observed on the entire printed mesh structures's surface. A similar self-wrinkling effect was observed by Chandra et al [22]. They suggested that this effect was mainly due to oxygen inhibition which caused crosslinking speed variation from the top to the bottom. When UV curable films were exposed to UV illumination within the presence of oxygen, a thin layer at the top surface will remain uncured due to the oxygen inhibition. A crosslink gradient would be formed through the depth direction because of oxygen concentration gradient formed at the surface by diffusion. This situation will lead to in-plane stress and cause surface wrinkle. In Chandra et al.'s work, they also concluded that by controlling the oxygen concentration in the environment, the size of surface wrinkle could also be controlled.

Figure 7 is a printed curving mesh structure with PCLDMA: PEGDA (70:30) ink. 50 layers were printed and surface profiling data Figure 7(d) showed the total height of the structure was around 250μm. Figure 8 shows optical microscopy images of a printed curving mesh structure. Similar effects were also observed that the ink did not fully cure immediately after deposition and droplets at the edges falling down to the substrate forming coarse structures at the base.

Conclusion

A PCLDMA: PEGDA ink that is suitable for 3D inkjet printing to produce biodegradable 3D structures has been demonstrated for the first time. For different printers, the proportion of PEGDA and processing temperature can be varied, which should be decided based on the given rheology database.

In this paper, PCLDMA: PEGDA (70:30) was chosen and observed to be suitable for a Dimatix DMP-2800 when printed at 60ºC. The prepared ink can be cured sufficiently to retain expected structures during printing and stable products can be produced. The hardness of printed samples was around 5MPa with an indentation modulus of 30MPa. These properties increased when a post-curing procedure was applied. However, only the mechanical properties at the top surface were improved. From SEM examination, it was found that print quality was influenced by curing speed and wrinkles were observed on the surface of the cured structures. For future work, the curing efficiency and printing qualities of PCLDMA:PEGDA (70:30) ink with different photo-initiator / accelerator ratios should be investigated. Oxygen inhibition effects will also be studied by performing printing under different oxygen concentration levels to investigate the impact on printing quality and mechanical properties of cured structure.

References

[1]Bobyn, J D ; Stackpool, G J ; Hacking, S A ; Tanzer, M ; Krygier, J J., *Characteristics Of Bone Ingrowth And Interface Mechanics Of A New Porous Tantalum Biomaterial*, ,The Journal Of Bone And Joint Surgery. British volume, 1999, Vol.81(5), pp.907-14

[2] Hacking, S. A., Bobyn, J. D., Toh, K.-K., Tanzer, M. &Krygier, J. J., *Fibrous Tissue Ingrowth And Attachment To Porous Tantalum*. *J. Biomed. Mater. Res.* 2002*,* 52, 631–638

[3] Bobyn, J. D., Pillar, R. M., Binnington, A. G. &Szivek, J. A.,*The Effect Of Proximally And Fully Porous-Coated Canine Hip Stem Design On Bone Modeling.*J. Orthop*. Res.* 2005*,* 5, 393–408.

[4] Ramanath H.S., Chua C.K. Leong K.F., Shah K.D., *Melt Flow Behaviour of Poly-ε-caprolactone in Fused Deposition Modelling,* J Mater Sci, 2008, 19, pp 2541-2550

[5] Pitt C.G., Schinder A., Capronor-A Biodegradable Delivery System for Levonorgestrel, Long-acting contraceptive systems, Harpen& Row, Philadephia (1984),pp. 48-63.

[6] Jiang C., Huang f., Hsieh M., *Fabrication of synthesized PCL-PEG-PCL tissue engineering scaffolds using an air pressure-aided deposition system,* Rapid Prototyping Journal,2011, vol17(4), pp288-297

[7] Williams, J.M., Adewumi A., Schek R.M., Flanagan C.L., *Bone Tissue Engineering using Polycaprolactone Scaffold Fabricated via Selective Laser Sintering,* Biomaterials, 2005, vol 26(23), pp 4817-4827.

[8] Eshraghi S., Das S., *Mechanical and Microstructural Properties of Polycaprolactone Scaffolds with One-dimensional, Two-dimensional and Three-*

dimensional Orthogonally Oriented Porous Architectures Produced by Selective Laser Sintering., ActaBiomaterialia, 2010, vol 6(7), pp. 2467-2476.

[9]Feng ZG et al, *Synthesis and characterization of biodegradable hydrogels based on photopolymerizable acrylate-terminated CL-PEG-CL macromers with supramolecular assemblies of a-cyclodextrins*, Polymer,2003, vol44,pp 5177–5186

[10]Park, JS et al, *In vitro and in vivo test of PEG/PCL-based hydrogel scaffold for cell delivery application*, Journal of Controlled Release, 2007, vol124, pp51–59

[11] Cuchiara P.C., Allen A.B., Chen T.M., Miller J.S., West J.L., *Multilayer microfluidic PEGDA hydrogels*, Biometerials, 2010, vol31, pp5491-5497

[12] Hahn, M.S., Taite L.J., Moon J.J. Rowland M.C., Ruffino K.A., West J.L., *Photolithographic patterning of polyethylene glycol hydrogels*, Biomaterials, 2006, vol27, pp 2519-2524.

[13] Hahn M.S., Miller J.S., West J.L., *Laser Scanning Lithography for Surface Micropatterning on Hydrogel,* Advanced Materials, 2005, vol 17, pp 2939-2942.

[14] Huang M.H., Hutmacher D.W., Schantz J., Vacanti C.A., Braud C., Vert M., *Degradation and cell culture studies on block copolymers prepared by ring opening polymerization of ε-caprolactone in the presence of poly(ethylene glycol)*, Wiley InterScience, 2004 published online.

[15] Jette K.K., Law D., Schmitt E.A., Kwon G.S., *Preparation and drug loading of Poly(Ethylene Glycol)-block-Poly(ε-caprolactone) micelles through the evaporation of cosolventazeotrope*., Pharmaceutical Research, 2004, vol21(7), pp1184-1191

[16] Ainsley C, Reos N, Derby B, *Freeform Fabrication by Controlled Droplet Deposition of Powder Filled Melts*, J Mater Sci, 2002, vol37, pp 3155-3161

[17] Wang D.H., *UV Curing Materials: Theory and Application*, 2001, Science Publisher

[18]Decker C., *Kinetic Study and New Applications of UV Radiation Curing*, Macromolecular Rapid Communications, 2002, vol23,pp1067-1093

[19] Norbury, A., Samuel, T., The recovery and sinking-in or piling up of material in the Brinell test, and the effect of these factors on the correlation of Brinell and certain other hardness tests, The Journal of the iron and steel institute, 1928, vol117,pp. 673-687

[20] Gardel M.L., Shin J.H., MacKintosh F.C., Mahadevan L., Matsidaora P., Weitz D.A., Elastic behaviour of cross-linked and bundled actin networks, Science, 2004, Vol 304(5675), pp. 1301-1305

[21] Coran, A.Y., Science and Technology of Rubber, F.R. Eirich,Ed., Academic Press, New York, 1978, pp. 292

[22] Chandra D., Crosby A.J., *Self-Wrinkling of UV cured polymer films*, Advanced Maerials,2011, vol23, pp3441-3445.

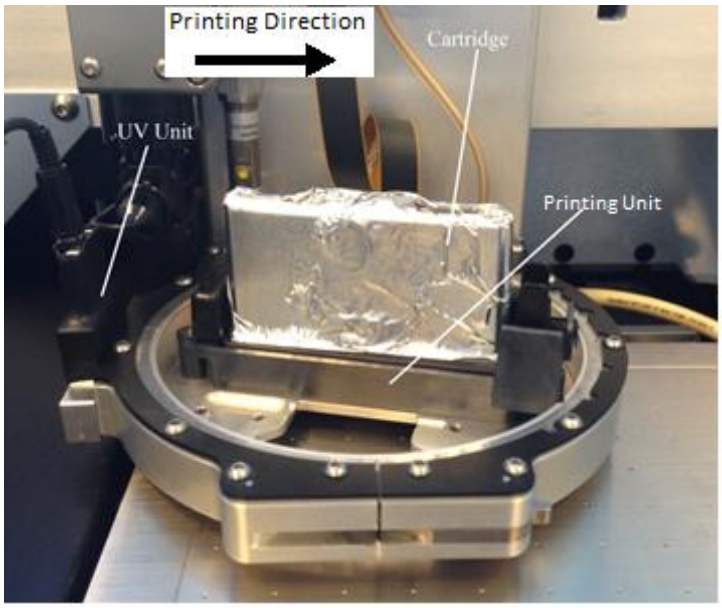

Figure1: Structure of printhead and UV curing unit.

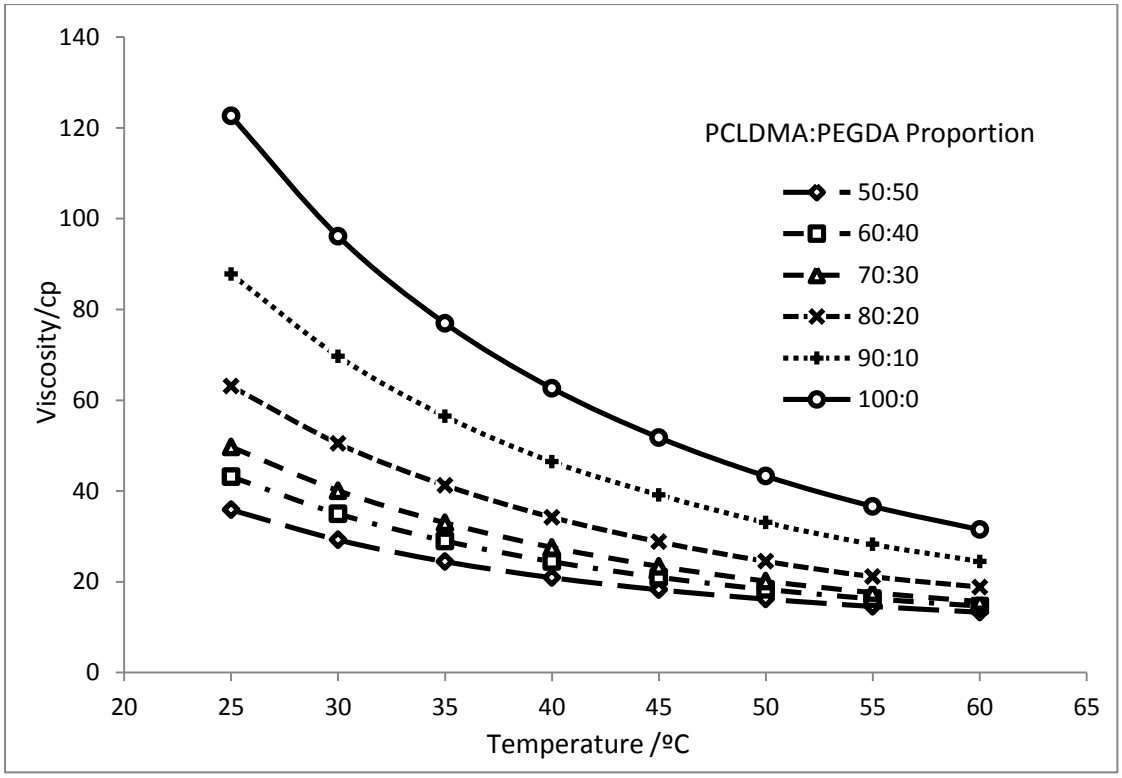

Figure 2: Viscosity distribution plot of PCLDMA: PEGDA with different proportions between 25 ºC to 60 ºC when shear rate equals to 1000s^{-}

(a)

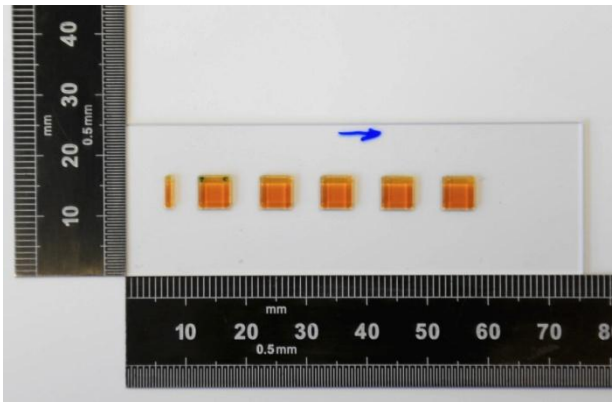

(b)

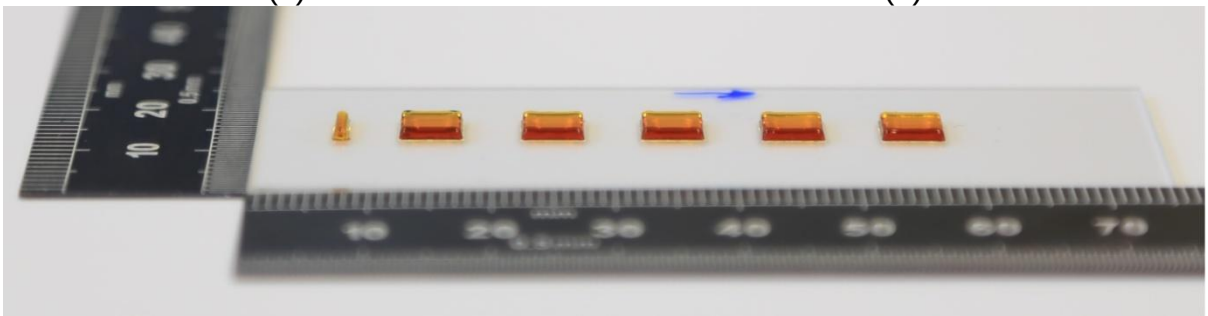

(c)

Figure 3 Printed square samples for nano-indentation test: (a) Printing pattern, (b) Top view of printed square samples, (c) Side view of printed square samples.

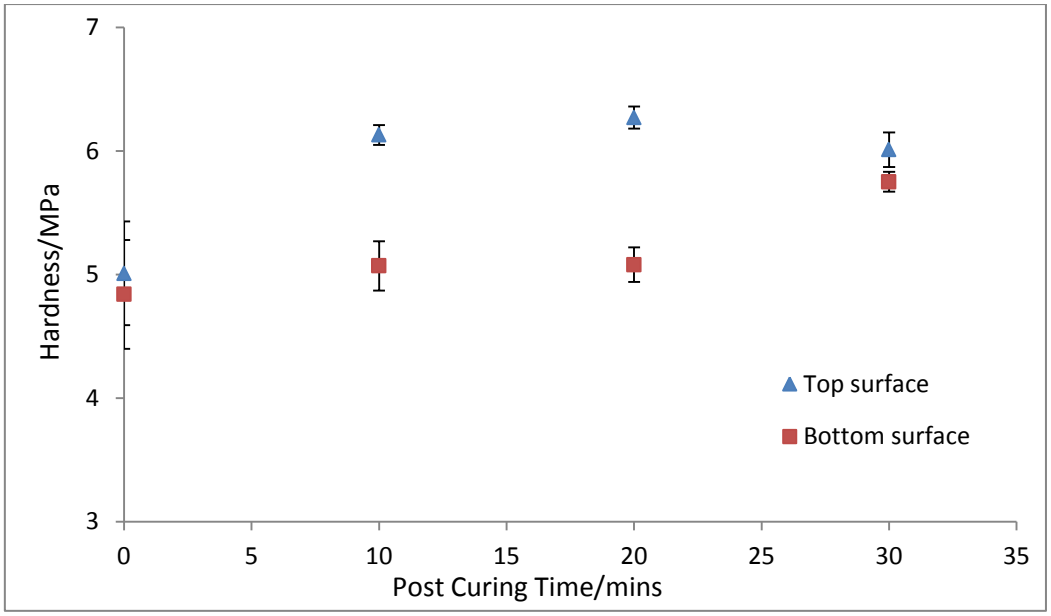

(a)

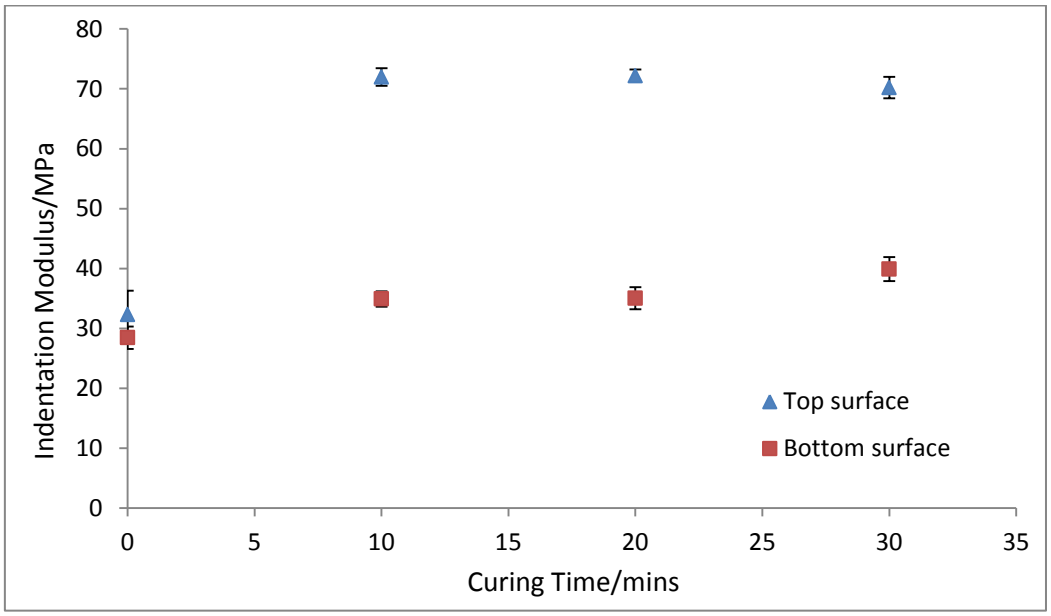

(b)

Figure 4:Plots of nanoindentation data for samples with different postcuring time. (a) Hardness, (b) Indentation modulus,

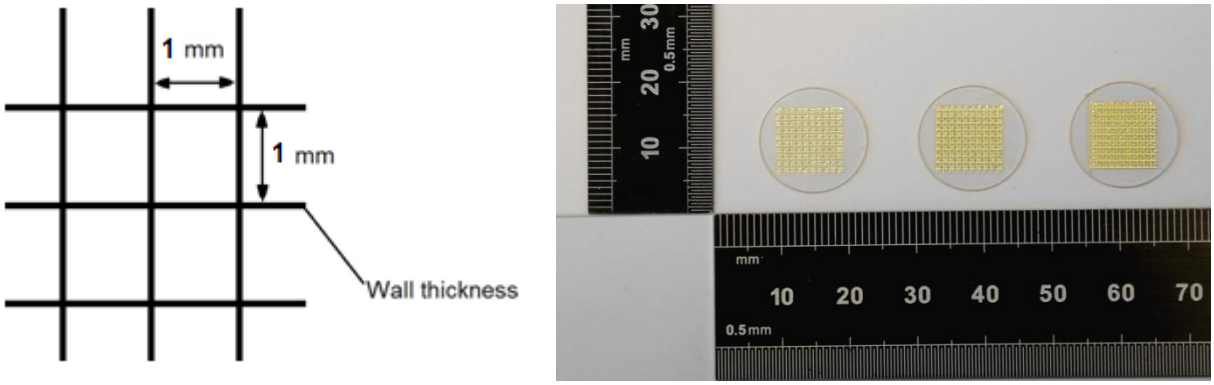

(a) (b)

Figure 5:Printed mesh samples for processing accurancy check (a) Schematic digram of printing pattern design (b) printed sample with different wall thickness (150μm, 300μm and 500μm from left to right)

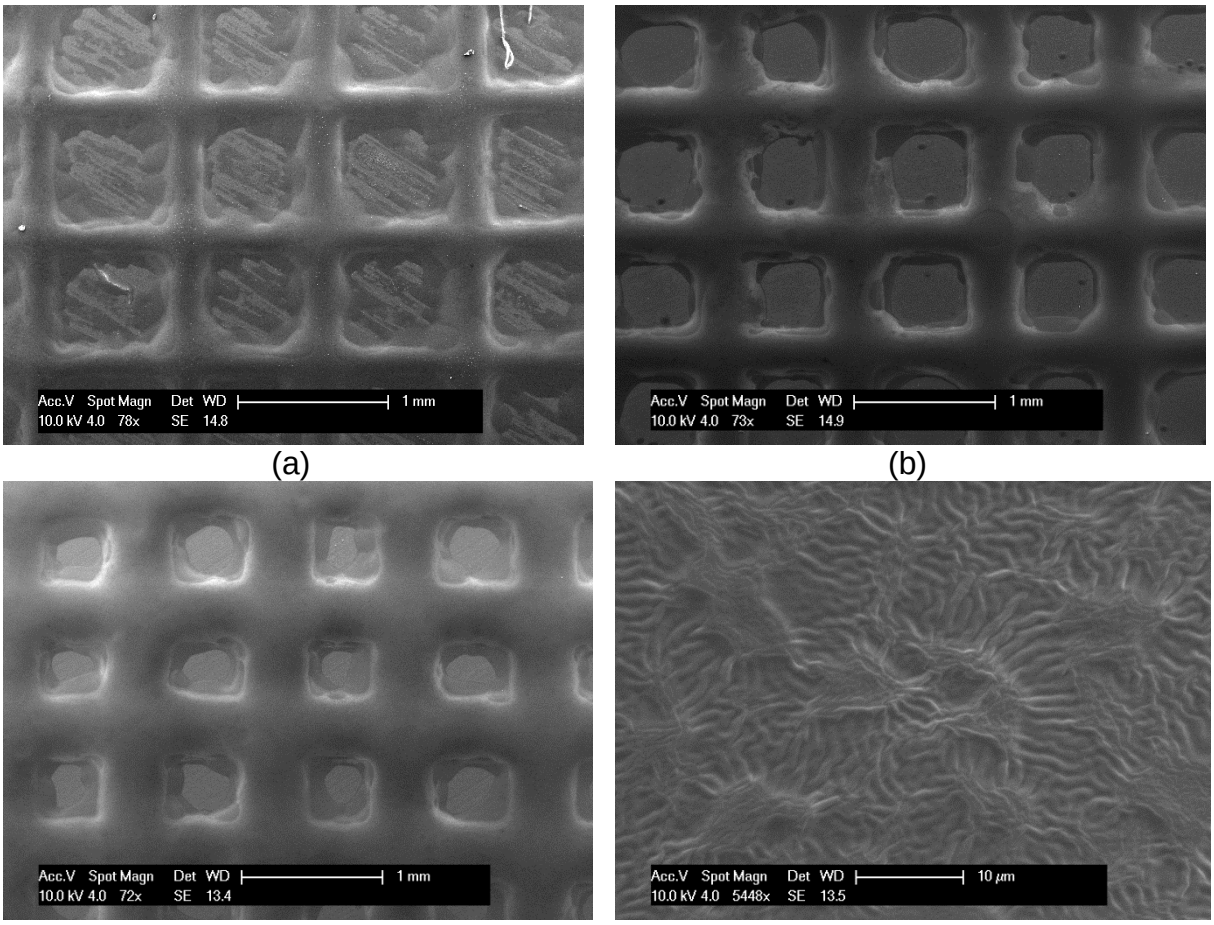

(a) (b)

(c) (d)

Figure 6: SEM pictures of printed mesh structure with different wall thickness: (a) 150μm, (b) 300μm, (c) 500μm, (d) winkle found at sample surface

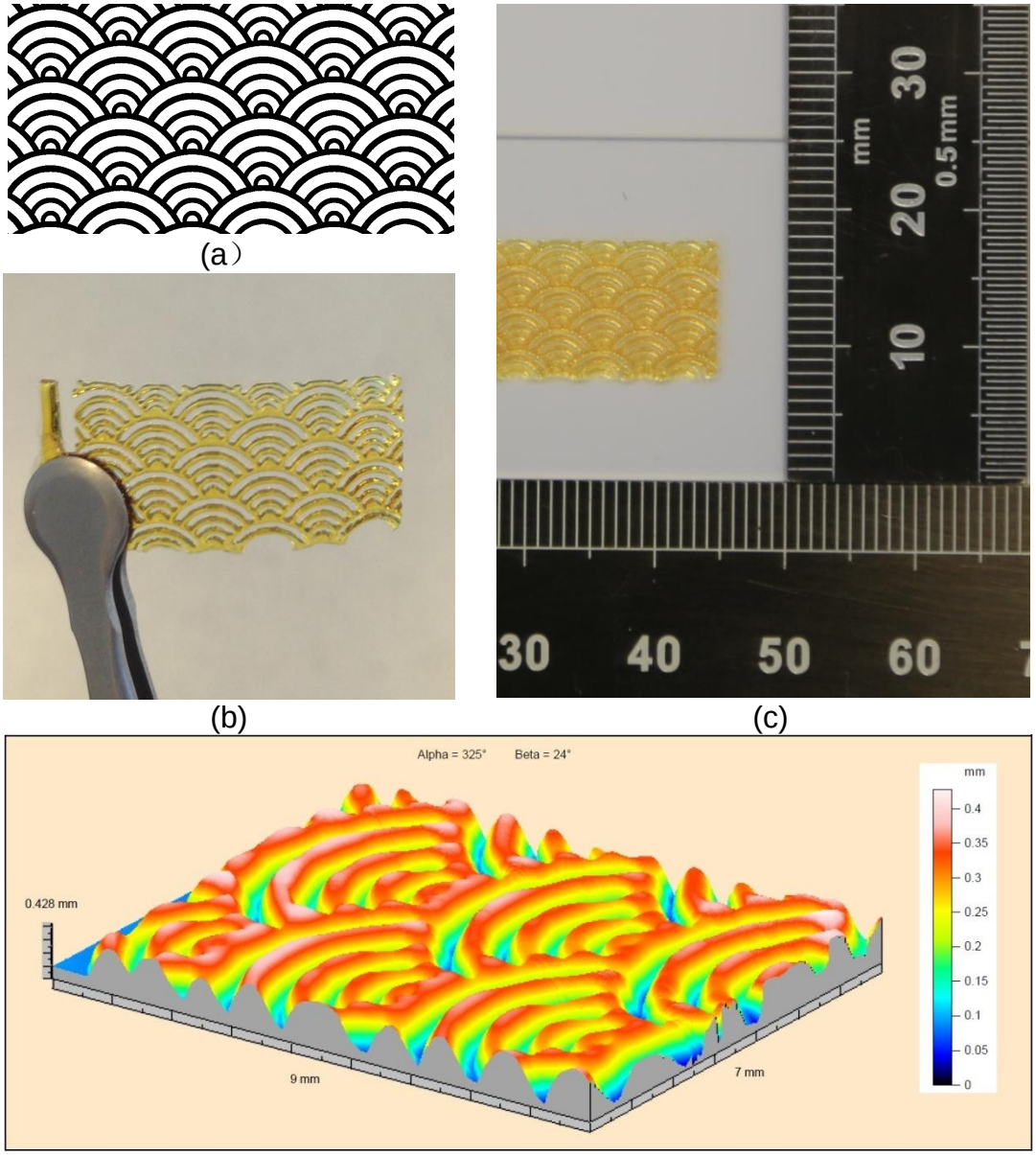

Figure 7: Curving mesh structure printing: (a) Printing pattern, (b) Sample appearance after taking off from glass slide, (c) Top view of printed sample, (d) Surface profiling of printed curving mesh structure

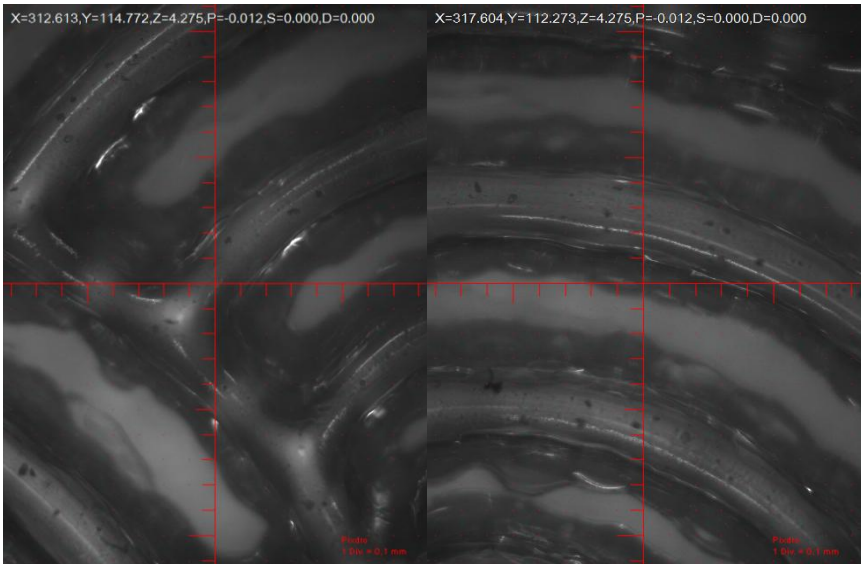

Figure 8: Microscopy pictures of printed curving mesh (1 division=100μm)

Table 1：Viscosity of PCLDMA: PEGDA with different proportions between 25 ºC to 60 ºC when shear rate equals to 1000s^{-1}

Temperature	PCLDMA:PEGDA Proportion					
	50:50	60:40	70:30	80:20	90:10	100:0
25 ºC	35.85±1.03	43.14±1.02	49.71±1.02	63.09±1.04	87.81±1.00	122.64±0.98
30 ºC	29.22±1.00	34.97±1.00	40.07±0.97	50.45±0.98	69.68±0.95	96.14±0.92
35 ºC	24.44±1.01	29.00±0.98	33.00±0.99	41.25±0.96	56.47±1.00	76.96±0.93
40 ºC	20.90±1.00	24.44±1.00	27.58±1.00	34.21±0.99	46.45±0.99	62.64±0.94
45 ºC	18.24±1.02	20.99±1.00	23.41±1.01	28.81±0.98	39.15±0.98	51.78±0.97
50 ºC	16.18±1.02	18.33±1.03	20.15±1.03	24.51±1.00	33.05±0.99	43.28±1.00
55 ºC	14.56±1.02	16.25±1.02	17.60±1.03	21.14±0.99	28.24±1.01	36.62±1.00

60 ºC	13.30±1.02	14.65±1.02	15.63±1.03	18.84±0.99	24.48±1.00	31.48±1.00

Table 2: Physical properties and printing indicator value of PCLDMA: PEGDA (70:30) mixture at temperature of 25ºC and 60 ºC

Temperature	Nozzle Diameter (μm)	Density (g/cm^3)	Viscosity (cp)	Surface Tension (mN/m)	PI (Oh^{-1})
25 ºC	21	1.08	49.71	37.26	0.58
60 ºC	21	1.08	15.63	32.31	1.73

Table 3: Viscosity monitoring of PCLDMA: PEGDA=70:30 sample between 55 ºC to 60 ºC when shear rate equals to $1000s^{-1}$

Temperature	PCLDMA:PEGDA=70:30		
	Without PI and AC	With PI and AC	With PI and AC degassed
50 ºC	20.15±1.03	20.44±1.02	22.27±1.01
55 ºC	17.60±1.03	18.35±1.01	19.54±1.01
60 ºC	15.63±1.03	16.57±1.02	17.55±1.04

Table 4: Hardness and indentation modulus for printed PCLDMA:PEGDA (70:30) before and after postcuring.

Curing Time		Hardness (MPa)	Indentation Modulus (MPa)
Top Surface	0min	5.01±0.42	32.28±3.99
	10mins	6.13±0.08	71.97±1.47
	20mins	6.27±0.09	72.17±1.04
	30mins	6.01±0.14	70.2±1.78
Bottom Surface	0mins	4.84±0.44	28.44±1.87
	10mins	5.07±0.20	34.90±1.27
	20mins	5.09±0.19	35.01±1.84
	30mins	5.75±0.08	39.88±2.01

Table 5: Comparison of actual printed wall thickness and designed wall thickness

Designed Wall Thickness	Printed Wall Thickness (Average)	Deviation (%)
150μm	194μm	29.3%
300μm	344μm	14.7%
500μm	463μm	-7.4%